IOP Publishing Nanotechnology
Nanotechnology 27 (2016) 355705 (6pp) doi:10.1088/0957-4484/27/35/355705

Promising thermoelectric properties of phosphorenes

Cem Sevik[1,3] **and Hâldun Sevinçli**[2]

[1] Department of Mechanical Engineering, Faculty of Engineering, Anadolu University, 26555, Eskişehir, Turkey
[2] Department of Materials Science and Engineering, Izmir Institute of Technology, Izmir, TR 35430, Turkey

E-mail: csevik@anadolu.edu.tr and haldunsevincli@iyte.edu.tr

Received 4 March 2016, revised 17 June 2016
Accepted for publication 20 June 2016
Published 25 July 2016

Abstract

Electronic, phononic, and thermoelectric transport properties of single layer black- and blue-phosphorene structures are investigated with first-principles based ballistic electron and phonon transport calculations employing hybrid functionals. The maximum values of room temperature thermoelectric figure of merit, *ZT* corresponding to armchair and zigzag directions of black-phosphorene, ∼0.5 and ∼0.25, are calculated as rather smaller than those obtained with first-principles based semiclassical Boltzmann transport theory calculations. On the other hand, the maximum value of room temperature *ZT* of blue-phosphorene is predicted to be substantially high and remarkable values as high as 2.5 are obtained for elevated temperatures. Besides the fact that these figures are obtained at the ballistic limit, our findings mark the strong possibility of high thermoelectric performance of blue-phosphorene in new generation thermoelectric applications.

Keywords: thermoelectricity, phosphorene, ballistic transport, thermal conductivity

(Some figures may appear in colour only in the online journal)

1. Introduction

Triggered by the realization of graphene, research on novel two-dimensional materials has become one of the major topics in materials science and condensed matter physics. New two-dimensional crystals have been investigated intensively [1] and several of them have been successfully fabricated, such as hexagonal boron nitride [2–4], silicene [5–8], and a large family of layered transition metal dichalcogenides [9–12]. Recently, a single layer of phosphorus, named as black-phosphorene (black-P) has been exfoliated [13, 14] and revealed as a new member of candidate materials for nanoelectronics applications [15–19] such as field-effect transistors [20, 21], wide-range photodetectors [22, 23], and high-performance lithium-ion batteries [24]. Following the experimental realization, other possible phosphorus based layered structures have been investigated and different stable allotropes have been determined by first-principles investigations [25–27]. Blue-phosphorene (blue-P) stands out among those as being the most stable structure, having only a few meV higher cohesive energy [27] than that of black-P.

Black-P was found to be a direct band-gap semiconductor with an estimated band gap of ∼2 eV [16] and its carrier mobility has been predicted to be as high as ∼1000 $cm^2V^{-1}s^{-1}$ [14]. In addition, as a result of first-principles based solution of the phonon Boltzmann transport equation, the room temperature lattice thermal conductivity, κ_L, of this material has been estimated in the range of 30 to 110 $Wm^{-1}K^{-1}$ and 13 to 36 $Wm^{-1}K^{-1}$ along zigzag (ZZ) and armchair (AC) directions [28–33] respectively. Due to such superior electronic transport properties and relatively low κ_L (compared with the κ of graphene, 2000 −5000 $Wm^{-1}K^{-1}$ [34]), black-P has been suggested as a potential material for new generation nano thermoelectric applications. As a matter of fact, the room temperature thermoelectric figure of merit (*ZT*) of two-dimensional and quasi-one-dimensional (ribbon) black-P have been estimated to be as high as 1.0 [28] and 6.4 [35] respectively, using the

[3] Author to whom any correspondence should be addressed.

semiclassical Boltzmann theory within the relaxation time approximation. In addition, a remarkable increase in the Seebeck coefficient and electrical conductivity of black-P with strain induced band convergence, which leads to a maximum room temperature *ZT* value ∼2.1 [36] have also been reported using the same method. However, as a result of first-principles calculations, Liao *et al* have revealed that the maximum room temperature *ZT* value is only around ∼0.06 [37]. On the other hand, the relatively high performance might be expected from blue-P and therefore it is worthwhile to shed light on its thermoelectric properties, as well. Besides these results on the thermoelectric performance of black-P, that of blue-P has not been investigated in detail yet.

We report ballistic transport calculations through which we investigate the performance limits of these materials and we compare and contrast the electronic, phononic, and thermoelectric transport properties of two types of single layer phosphorene structures, namely, black- and blue-phosphorenes. Our results for black-P are comparable with those previously reported by Liao *et al* [37]. On the other hand, quite efficient thermoelectric properties, even at moderate temperatures, are predicted for the blue-P structure, which suggest that blue-P is a strong candidate for future two-dimensional thermoelectric applications.

2. Method

The electronic properties and the interatomic force constants are obtained using the Vienna *ab initio* Simulation Package (VASP) [38, 39] which is based on density functional theory (DFT) [40–42]. The projector augmented wave pseudopotentials (PAW) [43, 44] from the standard distribution are incorporated in the calculations. For electronic exchange-correlation functional, the generalized gradient approximation (GGA) in its Perdew−Burke−Ernzerhof (PBE) parameterization [45] is used. In order to capture the effect of exchange-correlation energy functionals particularly on electronic transport properties, we also use the screened Heyd−Scuseria−Ernzerhof (HSE06) hybrid functionals [46], which mix GGA with the exchange from Hartree−Fock theory [47]. The vibrational frequencies are obtained by using PHONOPY code [48], which can directly use the force constants calculated by density functional perturbation theory [49] as implemented in the VASP code. Here, $4 \times 3 \times 1$ ($28 \times 24 \times 1$) and $5 \times 5 \times 1$ ($30 \times 30 \times 1$) conventional super cell structures (Γ centered k-points grids) are considered for black-P and blue-P respectively. A plane wave energy cut off and total energy convergence criterion of 500 eV is used in all simulations, while the force tolerance is set to 10^{-2} eVÅ^{-1}. To prevent spurious interaction between isolated layers, a vacuum spacing of at least 15 Å is introduced.

Vibrational thermal conductance is calculated from [50],

$$\kappa_{\mathrm{ph}} = \int \frac{\mathrm{d}\omega}{2\pi} \hbar\omega \frac{\partial f_{\mathrm{B}}(\omega, T)}{\partial T} \tau_{\mathrm{ph}}(\omega) \qquad (1)$$

where ω is the vibrational frequency, f_{B} stands for the Bose function, and τ_{ph} is the phonon transmission spectrum. In the case of the electrons, we use the functions [51],

$$L_n = -\frac{2}{h} \int \mathrm{d}E \frac{\partial f_F(E, \mu, T)}{\partial E} (E - \mu)^n \tau_{\mathrm{el}}(E) \qquad (2)$$

where n is integer, μ is the chemical potential, T is temperature, f_{F} is the Fermi function, and τ_{el} is the electronic transmission spectrum. Using L_n, the electrical conductance, Seebeck coefficient, and the electrical contribution to thermal conductance are calculated as $G = e^2 L_0$, $S = (L_1/L_0)/eT$ and $\kappa_{\mathrm{el}} = (L_2 - L_1^2/L_0)/T$ respectively. Accordingly, the power factor and thermoelectric figure of merit are predicted using $P = S^2 G$ and $ZT = S^2 GT/(\kappa_{\mathrm{el}} + \kappa_{\mathrm{ph}})$ respectively. In the ballistic limit, the transmission spectra can be obtained from the number of band crossings of a particular energy value. In order to obtain accurate results, 200×200 *k*-points for PBE and 100×100 *k*-points for HSE06 functionals are used to capture accurate electron transmission spectra. In addition, 100 *q*-points are used in the transverse direction to capture accurate phonon transmission spectra.

3. Results

Figure 1 shows the structural representation of in plane and out of plane views of black-P and blue-P crystals represented by rectangular and hexagonal primitive unit cells with the space groups D_{2h}^7 and D_{3h}^3, respectively. These structures with a nonzero intrinsic thickness differ in the arrangements of tetrahedrally coordinated P atoms in 2D lattice. The optimized first-principles lattice parameters, $a_1 = 3.34$ Å, and $a_2 = 4.62$ Å for black-P and $a_1 = 3.28$ Å for blue-P are in agreement with the previously reported values [21, 26, 27, 52].

The electronic properties of both materials are calculated using both PBE and HSE06 functionals as shown in figures 2(a) and (b). HSE06 functional results in a notable shift of the conduction bands, while the properties such as the group velocities and effective masses are not affected considerably. The determined HSE06 (PBE) band-gap values, 1.59 (0.91) eV for black-P and 2.73 (2.04) eV for blue-P are in quite good agreement with the previously reported values, 0.90 [26, 53] and 0.91 eV [13] PBE band gap for black-P, 1.50 [13] and 1.59 eV [53] HSE06 band gap for black-P, and 1.98 eV [27] PBE band gap for blue-P.

Before discussing the thermoelectric coefficients of phosphorenes, a few notes on their phononic properties are in order. The calculated results for the vibrational spectra of single layers of blue-P and black-P are depicted along the high symmetry *q*-points in figures 2(c) and (d). We predict quite similar frequency ranges reflecting the similar bonding characteristics of the two structures as previously reported [27]. The calculated phonon frequencies are free from imaginary frequencies over the whole *q*-space, which ensures the accurate determination of lattice thermal properties of the materials. Phonon dispersions of black-P along ZZ and AC directions display important differences. Acoustic modes of black-P have higher group velocities in the AC direction, but the number of modes are higher at lower energies in the ZZ

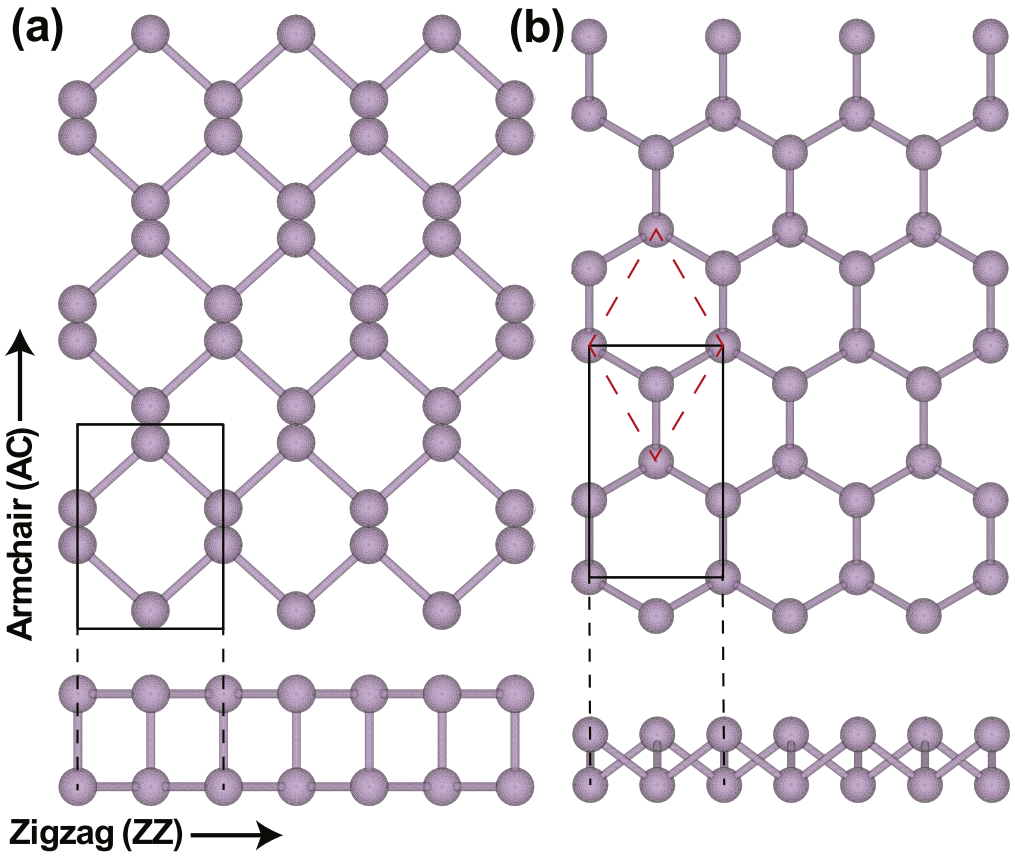

Figure 1. Schematic description of in plane and out of plane views of (a) black-P and (b) blue-P structures. The black tetragonal cells represent the conventional cells used in transport calculations and the red dashed cells represent the corresponding unit cell for blue-P.

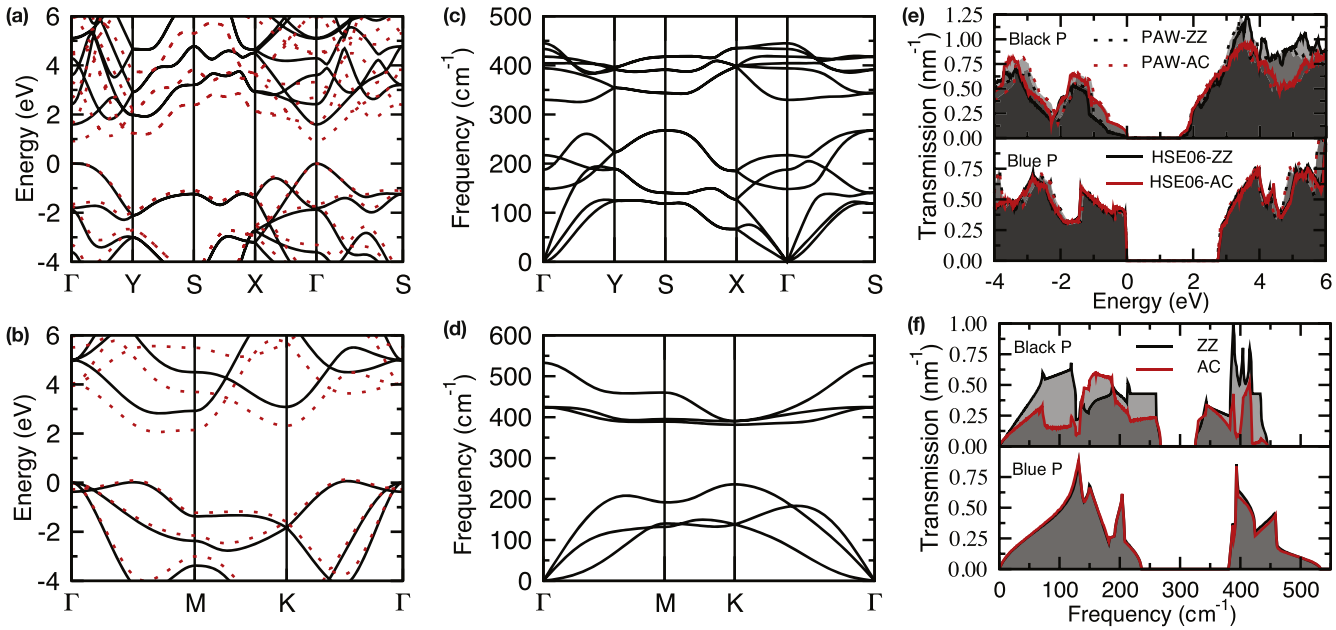

Figure 2. Electronic band structure of (a) black-P and (b) blue-P mono layers calculated using HSE06 (black solid lines) and PBE (red dotted lines) functionals. Vibrational band structure, $\omega(\mathbf{q})$ of (c) black-P and (d) blue-P mono layers. Ballistic electron (e) and phonon (f) transmission spectra of black-P and blue-P mono layers calculated by HSE06 (solid lines) and PBE (dotted lines) functionals. The black and red lines represent the transmission through zigzag (ZZ) and armchair (AC) directions, shown in figure 1, respectively.

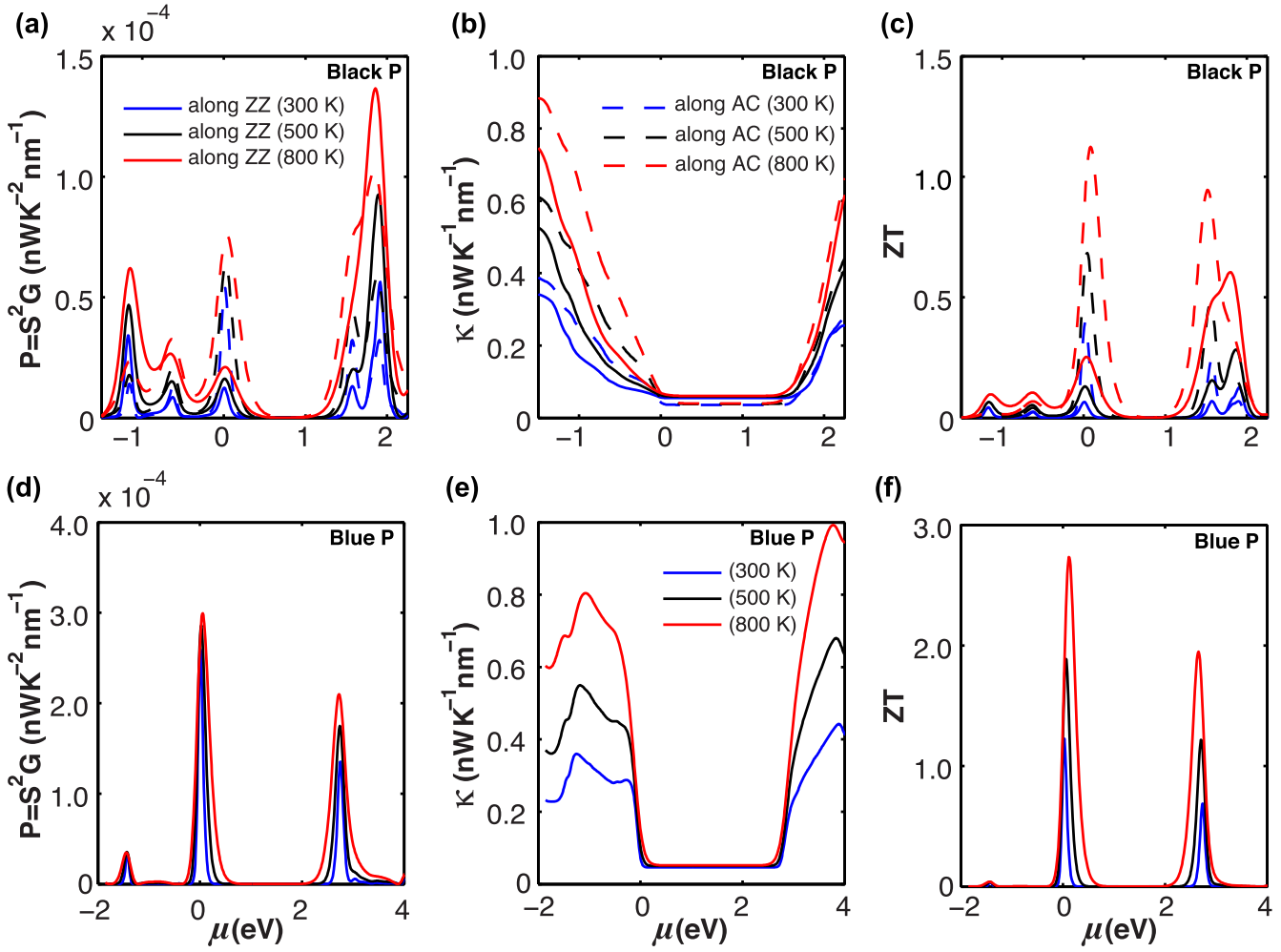

Figure 3. Thermoelectric coefficients of black-P and blue-P structures. The power factor $P = S^2G$, (a and d) electronic thermal conductance κ_{el}/A, (b and e) and ZT corresponding to the temperatures 300, 500, and 800 K (c and f). The labels ZZ and AC represent the armchair and zigzag directions shown in figure 1.

direction. As a result, phonon transmission is higher in the ZZ direction for low energy acoustic phonons up to ~150 cm^{-1}. Above 150 cm^{-1}, transmission is higher in the AC direction. Since the low energy phonons are dominant in thermal energy transport, we observe a higher κ_{ph} in the ZZ direction by a factor of 0.66, which is close to the values predicted previously with first-principles based solution of the phonon Boltzmann transport equation (0.45 [29] and 0.57 [32]) and non-equilibrium Green's function calculations (0.70 [30]). Both black-P and blue-P have phonon band gaps, starting at similar frequencies (30 meV), blue-P's band gap being larger by a factor of ~2.5 (19 meV). Such a band gap also has observable effects in thermal transport. At room temperature, black-P has 0.55 (0.35) nW K^{-1} nm^{-1} in the ZZ(AC) direction, while blue-P has 0.45 nW K^{-1} nm^{-1}. At 1000 K, these values are increased as 0.61 (0.40) and 0.52 nW K^{-1} nm^{-1}, respectively. Note that the maximum energies of the phonon modes correspond to 640 K and 780 K for black-P and blue-P respectively.

Electronic transmission spectra, τ_{el} calculated with both HSE06 and PBE functionals are given in figure 2(e) (The band gap values of two calculations are equalized). The electronic band structures of black-P and blue-P are quite different and this difference is reflected in their transmission spectra. In particular, transmission changes abruptly at the valence band edge of blue-P. This is a sign for high thermopower, which depends on the logarithmic derivative of the transmission function. In figure 3, we plot the power factor (P), thermal conductance ($\kappa = \kappa_{el} + \kappa_{ph}$) and thermoelectric figure of merit (ZT) for black-P and blue-P as functions of the chemical potentials at three different temperatures, T= 300, 500 and 800 K. Since the Seebeck coefficient is defined as $S = (L_1/L_0)/eT$, it returns extremely high but physically insignificant values inside the band gap. Power factor, $S^2G = L_1^2/L_0T^2$, yields purposeful results with a more direct connection to ZT. In figures 3(a), (d) power factors are shown as functions of chemical potential for black-P and blue-P respectively at different temperatures (300, 500, 800 K). Moreover, the maximum P values at the valence and conduction band edges are also reported in table 1. Indeed, these results are direct consequences of the transmission spectra of both structures.

Table 1. Calculated power factor values at close to the valence, P_V and conduction, P_C band edges, in units of pW K^{-2} nm^{-1} at different temperatures (300, 500, 800 K).

	Black-P ZZ		Black-P AC		Blue-P	
T	P_V	P_C	P_V	P_C	P_V	P_C
300	0.012	0.013	0.055	0.034	0.260	0.140
500	0.016	0.020	0.065	0.045	0.290	0.180
800	0.021	0.045	0.075	0.080	0.300	0.210

In figures 3(b) and (e) thermal conductance values are plotted as functions of the chemical potential at $T = 300$, 500 and 800 K. The values inside the band gaps are due to the phonons which are independent of the chemical potential. The relative contributions of electrons and phonons to thermal conductance is an indication of thermoelectric efficiency. If κ is dominated by the phononic contribution, most of the heat is transported without participating in electric current. In phosphorenes, κ is dominated by electrons unless μ is inside a band gap, which is an indication of high thermoelectric efficiency.

The resulting ZT values are plotted in figures 3(c) and (f) as functions of μ. The maxima are achieved in the proximity of the valence and conductance band edges. For black-P, $ZT = 0.13$ (0.4) is achieved in the ZZ (AC) direction at room temperature, while 0.6 (1.15) is possible at $T = 800$ K. These values are remarkably smaller than those predicted with the solution of *semiclassical* Boltzmann Transport equation (6.4 [35], and 2.1 [36]). However, our ballistic transport results are in parallel with the first-principles calculations considering the electron-phonon interaction in black-P based on density functional perturbation theory and Wannier interpolation (the maximum room temperature ZT values of p- and n-type black-P along armchair direction are around 0.06 and 0.04 respectively) [37]. Conversely, we predict quite high room temperature ZT values as high as 1.25 (0.7) valence (conduction) electrons of blue-P. Furthermore, significantly high ZT values (~2.5) is possible at elevated temperatures. The maximum ZT figures are plotted for black-P (ZZ and AC directions) and blue-P as functions of temperature in figure 4. One observes an almost linear dependence on temperature for all three plots, which indicates that Z are almost independent of temperature for phosphorenes.

In summary, our first-principles investigation explicitly states that previous calculations [28, 35, 36], treating the electron−phonon interaction with constant relaxation time approximation and estimating the electrical conductivity with deformation potential approximation, estimate the thermoelectric efficiency of black-P to be beyond their ballistic values. Thermoelectric efficiency sufficient for technological applications might be only possible at high temperatures for black-P. On the other hand, our ballistic quantum transport investigation conspicuously indicates the much better thermoelectric performance of blue-P. We attribute the rather higher maximum ZT values of blue-P to its high power factor resulting from the large slope in the transmission function around band edges, in agreement with the Mahan−Sofo criteria [54].

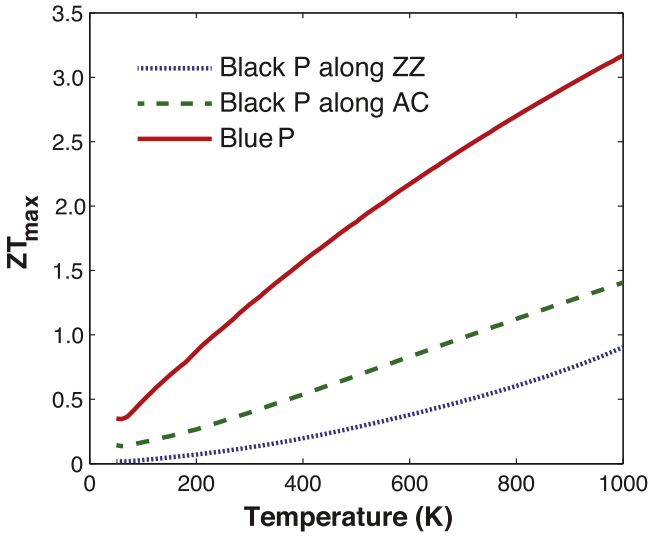

Figure 4. Maximum ZT as a function of temperatures corresponding to black-P and blue-P structures. The labels ZZ and AC represent the armchair and zigzag directions shown in figure 1.

Acknowledgments

We would like to thank the ULAKBIM High Performance and Grid Computing Center for a sufficient time allocation for our projects. C S acknowledges the support from Scientific and Technological Research Council of Turkey (TUBITAK-113F096), Anadolu University (BAP-140F335), and Turkish Academy of Sciences (TUBA-GEBIP). H S acknowledges support from Scientific and Technological Research Council of Turkey (BIDEB-113C032) and Bilim Akademisi-the Science Academy, Turkey under the BAGEP program.

References

[1] Miro P, Audiffred M and Heine T 2014 *Chem. Soc. Rev.* **43** 6537–54
[2] Zhi C, Bando Y, Tang C, Kuwahara H and Golberg D 2009 *Adv. Mater.* **21** 2889–93
[3] Zeng H, Zhi C, Zhang Z, Wei X, Wang X, Guo W, Bando Y and Golberg D 2010 *Nano Letters* **10** 5049–55
[4] Nag A, Raidongia K, Hembram K P S S, Datta R, Waghmare U V and Rao C N R 2010 *ACS Nano* **4** 1539–44
[5] Aufray B, Kara A, Vizzini S, Oughaddou H, Léandri C, Ealet B and Le Lay G 2010 *Appl. Phys. Lett.* **96** 183102
[6] Feng B, Ding Z, Meng S, Yao Y, He X, Cheng P, Chen L and Wu K 2012 *Nano Letters* **12** 3507–11
[7] Vogt P, De Padova P, Quaresima C, Avila J, Frantzeskakis E, Asensio M C, Resta A, Ealet B and Le Lay G 2012 *Phys. Rev. Lett.* **108** 155501
[8] Meng L *et al* 2013 *Nano Letters* **13** 685–90
[9] Wang Q H, Kalantar-Zadeh K, Kis A, Coleman J N and Strano M S 2012 *Nat Nano* **7** 699–712

[10] Radisavljevic B, Radenovic A, Brivio J, Giacometti V and Kis A 2011 *Nat Nano* **6** 147–50
[11] Chhowalla M, Liu Z and Zhang H 2015 *Chem. Soc. Rev.* **44** 2584–6
[12] Chia X, Eng A Y S, Ambrosi A, Tan S M and Pumera M 2015 *Chem. Rev.* **115** 11941
[13] Qiao J, Kong X, Hu Z X, Yang F and Ji W 2014 *Nat. Commun.* **5** 4475
[14] Li L, Yu Y, Ye G J, Ge Q, Ou X, Wu H, Feng D, Chen X H and Zhang Y 2014 *Nat. Nano* **9** 372–7
[15] Wang X, Jones A M, Seyler K L, Tran V, Jia Y, Zhao H, Wang H, Yang L, Xu X and Xia F 2015 *Nat. Nano* **10** 517–21
[16] Tran V, Soklaski R, Liang Y and Yang L 2014 *Phys. Rev.* B **89** 235319
[17] Xiao J, Long M, Zhang X, Ouyang J, Xu H and Gao Y 2015 *Sci. Rep.* **5** 9961
[18] Li X B, Guo P, Cao T F, Liu H, Lau W M and Liu L M 2015 *Sci. Rep.* **5** 10848
[19] Kim J S, Liu Y, Zhu W, Kim S, Wu D, Tao L, Dodabalapur A, Lai K and Akinwande D 2015 *Sci. Rep.* **5** 8989
[20] Liu H, Neal A T, Zhu Z, Luo Z, Xu X, Tománek D and Ye P D 2014 *ACS Nano* **8** 4033–41
[21] Fei R and Yang L 2014 *Nano Letters* **14** 2884–9
[22] Buscema M, Groenendijk D J, Blanter S I, Steele G A, van der Zant H S J and Castellanos-Gomez A 2014 *Nano Letters* **14** 3347–52
[23] Çakır D, Sahin H and Peeters F M 2014 *Phys. Rev.* B **90** 205421
[24] Li W, Yang Y, Zhang G and Zhang Y W 2015 *Nano Letters* **15** 1691–7
[25] Wu M, Fu H, Zhou L, Yao K and Zeng X C 2015 *Nano Letters* **15** 3557–62
[26] Guan J, Zhu Z and Tománek D 2014 *Phys. Rev. Lett.* **113** 046804
[27] Zhu Z and Tománek D 2014 *Phys. Rev. Lett.* **112** 176802
[28] Fei R, Faghaninia A, Soklaski R, Yan J A, Lo C and Yang L 2014 *Nano Letters* **14** 6393–9
[29] Qin G, Yan Q B, Qin Z, Yue S Y, Hu M and Su G 2015 *Phys. Chem. Chem. Phys.* **17** 4854–8
[30] Ong Z Y, Cai Y, Zhang G and Zhang Y W 2014 *J. Phys. Chem.* C **118** 25272–7
[31] Zhu L, Zhang G and Li B 2014 *Phys. Rev.* B **90** 214302
[32] Liu T H and Chang C C 2015 *Nanoscale* **7** 10648–54
[33] Jain A and McGaughey A J H 2015 *Sci. Rep.* **5** 8501
[34] Balandin A A 2011 *Nat. Mater* **10** 569–81
[35] Zhang J, Liu H J, Cheng L, Wei J, Liang J H, Fan D D, Shi J, Tang X F and Zhang Q J 2014 *Sci. Rep.* **4** 6452
[36] Lv H Y, Lu W J, Shao D F and Sun Y P 2014 *Phys. Rev.* B **90** 085433
[37] Liao B, Zhou J, Qiu B, Dresselhaus M S and Chen G 2015 *Phys. Rev.* B **91** 235419
[38] Kresse G and Hafner J 1993 *Phys. Rev.* B **47** 558–61
[39] Wu X, Vanderbilt D and Hamann D R 2005 *Phys. Rev.* B **72** 035105
[40] Kohn W and Sham L J 1965 *Phys. Rev.* **140** A1133–8
[41] Hohenberg P and Kohn W 1964 *Phys. Rev.* **136** B864–71
[42] Martin R M 2004 *Electronic Structure* (Cambridge, England: Cambridge University Press)
[43] Blöchl P E 1994 *Phys. Rev.* B **50** 17953–79
[44] Kresse G and Joubert D 1999 *Phys. Rev.* B **59** 1758–75
[45] Perdew J P, Burke K and Ernzerhof M 1996 *Phys. Rev. Lett.* **77** 3865–8
[46] Krukau A V, Vydrov O A, Izmaylov A F and Scuseria G E 2006 *J. Chem. Phys.* **125** 224106
[47] Becke A D 1993 *J. Chem. Phys.* **98** 1372–7
[48] Togo A, Oba F and Tanaka I 2008 *Phys. Rev.* B **78** 134106
[49] Baroni S, de Gironcoli S, Dal Corso A and Giannozzi P 2001 *Rev. Mod. Phys.* **73** 515–62
[50] Rego L G C and Kirczenow G 1998 *Phys. Rev. Lett.* **81** 232–5
[51] Esfarjani K, Zebarjadi M and Kawazoe Y 2006 *Phys. Rev.* B **73** 085406
[52] Aierken Y, Çakır D, Sevik C and Peeters F M 2015 *Phys. Rev.* B **92** 081408
[53] Çakır D, Sevik C and Peeters F M 2015 *Phys. Rev.* B **92** 165406
[54] Mahan G D and Sofo J O 1996 *Proc. Nat. Acad. Sci.* **93** 7436–9